JCSE The Journal of Corrosion Science and Engineering
ISSN 1466-8858 Volume 15, Preprint 32 submitted 7 July 2012

EIS Monitoring of Electrochemical Behavior of 304L Stainless Steel during Immersion in a diluted Nitric Acid Solution

N. Jahangiri, A.G. Raraz, J.E. Indacochea
Civil and Materials Engineering Department, University of Illinois at Chicago
and S.M. McDeavitt
Nuclear Engineering Department, Texas A&M University

Abstract

The passivation behavior of 304L stainless steel coupons in 5.0M HNO_3 was studied electrochemical impedance spectroscopy (EIS) and X-ray photoelectron spectroscopy (XPS). The electrical properties and compositional changes in the passive film with respect to immersion time are investigated by means of these two techniques.

EIS tests show progressive changes related to the formation and growth of a passive layer. An increase of resistance and decrease of capacitance values was observed when immersion time was extended. XPS spectra show that the passive layer is enriched in Cr oxide accompanied by the selective dissolution of Fe oxide with an increase in exposure time in the nitric acid solution.

Keywords

304L stainless steel, passive films, EIS, XPS

Introduction

It is known that stainless steels are spontaneously covered in oxygen-bearer environments by a protective chromium oxide passive film on their surfaces due to their chromium contents [1]. The chromium-rich oxide layer is very robust and durable; it is estimated that this passive film has a thickness of less than 5 nanometer or 15 layers of atoms, but it provides a high corrosion resistance [2-6]. C. Olsson et al. [7] reviewed the influence of different parameters on the formation of passive films. Among their findings, they determined that the passivation films are constantly changing and adapting to the environment to which the stainless steels are exposed. This means that the passive film can grow or dissolve, and may adsorb or incorporate anions related to the atmospheres they are exposed to. Besides, they indicated that a critical parameter to the stability of a passive film is related to the time the stainless steel surface needs to adapt to an environmental change.

Austenitic stainless steels are extensively used as structural materials for conditions where the component is exposed to nitric acid media [8]. AISI Type 304L stainless steel is the primary material utilized for construction of nuclear fuel reprocessing plants which handle nitric acid [9-10]. The major goal in our project is the evaluation of the corrosion behavior of an annular centrifugal contactor used in the Advanced Uranium Extraction (UREX+) process developed for the separation of uranium from the nuclear waste. Our study is directed on using the 304L SS as the structural material. In the present manuscript we are focusing on the formation and characterization of the passivation film of 304L when exposed to nitric acid. In this study, the

corrosion tests were undertaken in a 5.0M HNO_3 solution because this type of mix is used in the UREX+ procedure. The relationship between the corrosion resistance of 304L stainless steel in nitric acid solution and the immersion time has been investigated and the changes in the passive film are discussed.

Electrochemical Impedance Spectroscopy (EIS) and X-ray photoelectron spectroscopy (XPS) are surface sensitive methods that are frequently employed to study the passive films [11-12]. The non-destructive nature of EIS makes it a useful technique when electrochemical changes are studied as a function of time [13]; it provides a means of real time measurements of the formation and stability of protective oxide scales. XPS, which allows determining the chemical state of near-surface elements, is a valuable technique used to evaluate the corrosion resistance of stainless steels [3,14]. EIS and XPS techniques have been used in this study to investigate the changes in the passive film.

Experimental Procedure

The electrochemical tests were carried out in a three-electrode cell. The working electrode was Type 304L SS sample of wt. % composition 18Cr, 8Ni, 0.02C, 1.76Mn, 0.45Si, 0.3Mo. The working electrode had a surface area of 1.0 cm^2; its surface was grinded and polished to a 1 µm surface finish and thoroughly cleaned before being inserted in a Teflon specimen holder. A saturated calomel electrode (SCE) and a pair of graphite rods were used as the reference and counter electrodes, respectively. The solutions of 5.0M HNO_3 were prepared with distilled and deionized water and nitric acid of pure analytic grade. No attempt was made to deaerate the solutions prior their use.

The acidic solutions were prepared 2 hours prior to the immersion tests. The samples were immersed in the solution immediately after polishing and cleaning with methanol in order to minimize the amount of oxide film formed in air. The open circuit potential (OCP) was monitored with respect to time for a 10 second period before EIS. The EIS tests were carried out after the samples were immersed for 5 min and 0.25, 0.5, 1, 2, 4, 10, 24, 72, 96 and 120 hours.

The EIS tests were conducted using a computer-controlled Gamry PCI 4 potentiostat-galvanostat unit in a frequency range from 100,000 to 0.01 Hz, with signal amplitude of 10mV. The Zsimpwin 3.20 software was employed to acquire the values of the electrochemical parameters and further data analyses.

The XPS analyses were performed with a Kratos Axis-165 XPS instrument, using a monochromatized Al K-alpha x-ray source ($h \cdot \nu$=1486.7eV). Survey scans were conducted using pass energy of 160eV, while narrow scans were conducted using pass energy of 20eV. The binding energy scale was adjusted against the C(1s) peak at 284.5eV. Spectra of C, Fe, Cr, and Ni were recorded. The spectra obtained were fitted, after background subtraction, following the Shirley procedure with Gaussian-Lorentzian curves using XPSPeak 4.1 software.

Results and Discussion

Open-circuit Potential

Open-circuit potential (OCP) values were recorded for 10 seconds and their average values are presented in Fig. 1. It is observed that the increase in the immersion time leads to increase in the OCP. The time to reach stabilization is about 3 days and after that, the OCP values do not change significantly.

ISSN 1466-8858 Volume 15, Preprint 32 submitted 7 July 2012

The OCP values become more positive with time, which suggests that the film formed on the surface of stainless steel coupons prior to immersion is too thin to provide complete passivity and their immersion in the nitric acid leads to thickening of the passive film, and a nobler behavior. The relatively constant OCP values after about 90 hours of immersion suggest that a steady state condition is achieved.

Electrochemical Impedance Spectroscopy

Electrochemical impedance spectra were collected for different immersion time periods to understand the effect of exposure time on the development of the passive film and its electrochemical behavior. Bode-magnitude plots were generated and are presented in Fig. 2. Three distinct regions can be identified; at high frequencies (~10-100 kHz), all curves go flat (slope ~ 0) regardless of their immersion time (Fig. 2a). This type of behavior is attributed to the ohmic resistance of the electrolyte. At the moderate frequencies, the spectra display a negative linear slope (~ -1), which is the characteristic response of a capacitive behavior of a passive film. At low frequencies (< 0.1 Hz), the spectra display a considerable decrease in impedance values at short immersion times, as seen in Fig. 2b; this concurs with the formation of the passive layer, that is expected to bring in a resistive factor. This change from capacitive to resistive behavior becomes less noticeable at longer immersion times (> 3 days); for these longer immersion times, the impedances tend to keep their capacitive behavior by staying aligned to the linear slope (~ -1). In the shorter immersion times, the deviation from the capacitive behavior is significant and this is correlated with the dissolution of ions. But then with increasing immersion times the protective passive film, that will become thicker, lowers the dissolution rate.

The Bode phase plots in Fig. 3 also show three different regions. At high frequencies there is overlapping within the impedance spectra, and the phase angle values are in the range of -3 to -10°. The reason for the phase angle value being greater than zero is due to the electrolyte resistance (R_s). At the middle frequency range, the phase angle reaches values below -80° indicating presence of a passive film that shows a near capacitive response; a phase angle of -90° represents a pure capacitive behavior [15]. It is also observed at this frequency range, that the lengths of the lines in the broad plateau above -80° increase as the immersion times become longer. At frequencies less than 1 Hz, when the immersion times are reduced the changes in phase angle get larger transitioning from the middle to the lowest frequencies. For the shortest immersion times (≤2 hours), the spectra deviate considerably downward from -80° (Zphase ~ -10° to -30°); indicating that the effect of dissolution (corrosion reaction) is more clearly defined. Although corrosion is occurring, the protective passive film that develops continuous to grow with longer immersion times, since the phase angle decreases; but the passive film is still thin. For the immersion times of 4 to 24 hours the Zphase angle reduces between -40° and -60°, anticipating a thicker and more protective passive layer. But then for the immersion times of 3, 4, and 5 days the phase angle remains at ~ -70° (at 10^{-2} Hz), signifying a more robust, thick, stable, and very protective passive film. This results in very low ion dissolution rates.

A Nyquist plot relates the real component of the impedance with the imaginary component of the impedance in decreasing frequency. The Nyquist plots for this study are given in Fig. 4; all of them can be described as large depressed semicircles and the diameters of these semicircles become larger as the immersion time increases. This type of impedance spectra that show a nobler electrochemical behavior with time suggest charge transfer controlled corrosion processes, which can be caused by the build up of passive films of specific compositions and with selective dissolution of some ions. It is observed in Fig. 4 that the Nyquist plots

corresponding to the samples immersed for 2 hours or less appear to have pulled together having almost half the semicircle completed. The second set of plots corresponds to coupons immersed between 4 and 24 hours. The Nyquist plots for the coupons immersed for 3, 4, and 5 days are clearly together. These differences were also noted in Figs. 2-3 and mentioned in our previous discussion. Such variations may suggest different corrosion reactions with immersion time or perhaps differences in the corrosion film size and composition, that would delay the charge transfer and hence slow down the corrosion rate until reaching a robust and stable passive film.

Based on this particular behavior, the electrical circuit model known as Randles cell (Fig. 5) was selected to carry out the curve fittings which appear as solid lines in Fig. 4; a good fitting of the experimental results is observed. This equivalent circuit model establishes that the solution acts as a resistor (R_s), and the oxide (passive) film has a capacitance (CPE), and resistance (R_{pf}) components. The later is known as polarization resistance. Fitting the EIS experimental spectra by the circuit model allows the calculation of the electrical components which are presented in Table 1. R_s corresponds to the ohmic resistance of the electrolyte, and it depends on electrode and cell geometry [16]. R_{pf} represents the resistance of the passive film due to its ionic conductivity. The CPE is the constant phase element, and it represents the capacitance parameter of the passive film due to its dielectric parameters [17]. The R_{pf} is in parallel with the CPE, and both are in series with the R_s. The CPEs can be used in empirical models and it causes a rotation of the center of the capacitive semicircle below the real axes by a frequency independent constant phase angle, Φ:

$$\Phi = \frac{(1-n)\pi}{2} \qquad (1)$$

where n shows the deviation of the CPE from the ideal capacitances (n=1). Therefore, replacing the capacitance by CPE provides the advantage of obtaining better fittings. The impedance related to the CPE can be given by:

$$Z_{CPE} = Q_{pf}^{-1} \cdot (j\omega)^{-n} \qquad (2)$$

where Q_{pf} is the CPE parameter, j is the imaginary constant and ω is the radial frequency and as mentioned before, n shows the phase shift. The total impedance of the Randles circuit, Z_{total}, is described by the following expression [18-20]:

$$Z_{total} = R_s + \left[\frac{1}{R_{PF}} Q\omega^n (\cos\frac{n\pi}{2} + j\sin\frac{n\pi}{2}) \right]^{-1} \qquad (3)$$

Correlation of EIS Fitted Data with Passive Film Formation and Growth

The information presented in Table 1 shows the electrolyte resistance (R_s) with no meaningful changes, but R_{pf} and Q_{pf} values which are related to the passive film development and growth experience changes with immersion time. Both of these parameters were plotted as function of the time of immersion, as shown in Fig. 6. The changes in the passive film resistance, R_{pf} can be observed in Fig. 6a. Three regions are distinguishable which are shown in the graph with straight

lines superimposed on the fitting curve. The five data points corresponding to the resistances of the samples exposed for 2 hours or less, signal immediate development of the passive film, as the R_{pf} increases from about 40.0 kΩ/cm^2 to about 200.0 kΩ/cm^2; such increase in resistance must be accompanied by the thickening of the passive film, as related by the equation:

$$R_{pf} = \rho \cdot \frac{d}{A} \qquad (4)$$

where ρ is the resistivity of the oxide film, d is the thickness, and A is the effective surface area. At this stage, however, the oxide film is still too thin to significantly slow down the corrosion rate, as reflected by the slope of the initial straight line. But then at the intermediate times of 4 to 24 hours, the R_{pf} increases at a slower rate suggesting a change in the thickness of the passive film but not as quick. The passive film resistance becomes constant for immersion times greater than 3 days at a mean value of 1.125x10^6 Ω/cm^2. Obviously, the passive film has reached a critical thickness, which brings the corrosion of the stainless steel coupons to a virtual stop. Note that in Fig. 6a, an immersion time of about 90 hours was extrapolated that corresponds to the average passive film resistance. It is important to point out that this critical time is similar to the time that takes the OCP to reach stabilization (Fig. 1).

The capacitance parameter, Q_{pf}, was also plotted as function of immersion time (Fig. 6b), and these values decrease with increases in immersion time. Alike the results presented in Fig. 6a, three distinct regions are identified that show a rate change of the Q_{pf}. The rate change becomes zero in the samples exposed to 3, 4, and 5 days. It has been explained that the capacitance value is inversely proportional to the thickness of the passive layer [21]. The capacitance is also related the thickness of the passive layer for a homogenous oxide film according to the equation:

$$C = \varepsilon\varepsilon_0 \cdot \frac{A}{d} \qquad (5)$$

where C is the capacitance, d the oxide film thickness , A the effective surface area, ε the dielectric constant, and ε_0 the permittivity of vacuum ($8.85\times10^{-14} F/cm^{-1}$) [13,22]. Since n is close to unity (n ~ 0.94 - 0.95), as seen in Table 1, this suggests that the film is homogenous, and hence would behave like an ideal capacitor [22-23].Consequently, the decrease in the Q_{pf}, values with time is a sign of the growth of the passivation film on surface of 304L stainless steel.

Compositional Changes of the Passive Film

The electrochemical impedance spectroscopy (EIS) results discussed above, demonstrated the formation and progress of the passive layer, where three different regions were identified as shown in Fig. 2-3,6. X-Ray Photoelectron Spectroscopy (XPS) analyses were performed on selected samples corresponding to each of these stages to see if the changes noted in the passive film electrical properties and thickness go together with compositional variations. High-resolution XPS spectra were used to analyze Cr, Fe, and Ni as elements and the forming oxides. Iterative fitting was used to obtain the proper fitting of the experimental data. The NIST Standard Reference Database [24] was used to match the peaks in the XPS spectra. Quantitative analysis of XPS spectra based on the peak areas, and considering $2p_{3/2}$ resolutions, was used to investigate the effect of immersion time on the characteristics of the passive film.

ISSN 1466-8858 Volume 15, Preprint 32 submitted 7 July 2012

Fig. 7 shows Cr and Fe XPS spectra for all five samples. An increase in the chromium and oxygen peak intensities was observed along with a relative reduction of the iron peak intensity with longer immersion times. Fig. 8 depicts the compositional changes of Cr and Fe as function of time within the protective layer. Cr showed only a small intensity increase initially, after 5 and 15 minutes exposure, compared to the as-polished sample; however, it almost doubled with the 24-hour immersion, and it leveled off in the sample immersed for 5 days. On the other hand, the Fe content in the passive film decreased rapidly after the 5 and 15 minute exposure compared to the as-polished sample; it flattened out after a 24 hour of immersion and remained constant in the 5-day exposure. It is evident that the compositional changes in the passive film do correlate with the EIS results. Note that in the short immersion times of 5 and 15 minutes, the build up of Cr in the passive layer is minor (Cr(ox)/Cr(met)), while Fe drops significantly (Fe(ox)/Fe(met)); this suggests that Fe is selectively dissolved, because Fe diffuses faster than Cr within the passive layer [25]. It has been mentioned that a passive layer formed in HNO_3 solutions is rich in Cr_2O_3 by dissolving more of the exogenous iron and iron oxides from stainless steel surfaces [26-27]. Moreover, the initial passive film is thin and perhaps more permeable at these early stages and it allows corrosion to proceed. In the 24-hour immersion sample, which corresponds to stage 2 (Fig. 6), a significant increase in the intensity of Cr(ox)/Cr(met) is observed, almost doubled. The intensity of Fe(ox)/Fe(met) XPS spectrum shows a much smaller decrease, which indicates a slower dissolution rate of Fe; this implies that the passive film, at this point in time, is being enriched in chromium and becomes more impermeable to corrosion agents as it grows denser and thicker. In stage 3, Fig. 8 shows that the intensities of Cr and Fe plateau suggesting a stable, impermeable, and robust passive film that lowers corrosion significantly.

It has been reported that whereas passive film formation and growth occurs in seconds or minutes, ordering (long range) within the film occurs at considerably much sluggish rates that takes several hours [7]. Our investigation correlates with such reports, it is evident that a passive layer is formed immediately upon exposure to the 5.0M HNO_3 solution and it increases at a fast rate within the first two hours of exposure (stage 1, Fig. 6). It should be mentioned that the stainless steel would already have a thin passive layer before any corrosion test, due to the exposure of the coupon to the ambient. It is in stage 2, for samples exposed to 4, 10 and 24 hours, were the changes in the passive layer (thickness and density) are slowed down, and become lethargic for exposures of 3 days and longer (stage 3).

Fig. 9 shows the Ni 2p spectra for the as-polished sample and samples immersed in the 5.0M HNO_3 for 5 minutes, 15 minutes, 1 day and 5 days. The as-polished sample shows $Ni2p_{3/2}$ in both metallic and oxide state. However, the spectra for the Ni oxide disappear after the sample is exposed to the acid. After immersion, the intensity of Ni peak decreases slightly as the data present in Table 2 indicates. The absence of Ni oxide peak in the spectra of immersed samples implies selective dissolution of Ni oxide after exposure to nitric acid. This is in agreement with the literature which indicates that the passive film of stainless steels containing nickel does not include oxidized Ni in a detectable amount [11, 28].

Passive Film Formation and Growth Mechanism

The protective passive film development followed the analysis of the corrosion results in our investigation may be considered to be controlled by two mechanisms which occur in sequence: 1) initial composition changes within an already existent passive Cr_2O_3 film which is thin and porous, and it is governed by the rapid dissolution of iron through the pores or micro-pores and a

simultaneous increase in Cr_2O_3 content, but at a much slower pace; and 2) the densification and growth of the passive layer which is expected to consist mainly of Cr_2O_3 and it will limit the Fe dissolution. The formation of the passive film can be related to the thermodynamic affinity of chromium to oxygen to form Cr_2O_3, its stability, and its chemical inertness [29-30].

The impedance characteristic of a passive film has three components, as indicated in equation (6), that are connected in series and the total impedance is controlled by the impedance component with greater magnitude [29]:

$$Z_T = Z_{m/f} + Z_f + Z_{f/s} \quad (6)$$

where; Z_T is the total impedance; $Z_{m/f}$ is the impedance at the metal/film interface; Z_f the impedance of the film; and $Z_{f/s}$ the impedance of the film/solution interface. Based on our experimental results and analysis, it is expected that Z_f is the main impedance component of the protective passive film. This last component could be is taking into account to hypothesize the model to explain the passive film formation and growth. As indicated earlier, the passive film resistance tended to increase at a fast rate for short exposure times (< 2 hours), but the magnitudes were still low (Fig. 6a); this suggests that the thickness of the film was still thin and not as dense to protect the stainless steel from corrosion, as described in Eq. (4). However, the longer exposure times resulted in thicker and denser film with greater corrosion protection, which correlated with increases in R_{pf} (Fig. 6a). It is evident from this plot that the polarization resistance is low at the beginning, and increases rapidly within the first 2 hours; this 1st stage is controlled by the dissolution of Fe, where the level of Fe in the film decreases suddenly and the increase of Cr in the passive film is very small, as seen in Fig. 8. The 2nd stage is accompanied by slower Fe dissolution rates and moderate increases in the levels of Cr in the passive film, but at reduced rates for times of 4 to about 24 hours. It is apparent that at this stage the thickness and density of the passive film is greater than stage 1; this corresponds to the increases in R_{pf} but also at reduced rates (Fig. 6a). It is at the 3rd stage where the system reaches stability; here the levels of Fe and Cr in the film remain constant, the R_{pf} stays constant, as well as the corrosion rate.

4. Conclusions

- The corrosion of 304L SS samples in aerated HNO_3 solutions at room temperature leads to the formation of a protective passive film. EIS provided the instantaneous changes in the electrical properties of the passive film, as well as its protective ability depending on the exposure time.
- Longer exposure times increased the passive film resistance (R_{pf}) and CPE values due to a high Cr content in the passive layer and increased film thickness. Both of the CPE and R_{pf} values become approximately constant after 3 days of immersion.
- The formation of the dynamic protective passive film suggests that it consists of three sequential stages characterized by three corrosion rates. The first stage shows relatively large corrosion rates, which involves mainly the dissolution of iron and slight Cr enrichment of a thin passive film. The second stage corresponds to a thicker and denser passive film with higher levels of Cr and diminished Fe concentrations, and reduced corrosion rates. In the third stage the densification and growth of the passive film is completed; the Cr concentration reaches a maximum and levels off, while Fe content is

minimum and constant. The corrosion rate at this last stage is at a minimum and stays unchanged. The XPS data showed that the compositional changes in the passive film corresponded to the three mentioned stages of the passive film formation and growth.

Acknowledgements

This investigation is supported by the U.S. Department of Energy, Nuclear Energy Research Initiative - Award No. DE-FC07- 07ID14890 Project No. 08-039 (UIC Grant # 493228).

References

1. B. D. Craig, Handbook of Corrosion Data, 2nd Edition, ASM International, Ohio, USA, 1995.
2. W. Lai, W. Zhao, F. Wang, C. Qi, J. Zhang, Surf. Interface Anal. 2009, 41, 531.
3. S. J. Kerber, J. Tverberg, Adv. Mater. Process. 2000, 11, 33.
4. J. Yuan, S. O. Pehkonen, Y. P. Ting, E. T. Kang, K. G. Neoh, Ind. Eng. Chem. 2008, 47, 3008.
5. L. Hamadou, A. Kadri, N. Benbrahim, J-P. Petit, J. Electrochem. Soc. 2007, 154, G291.
6. R. R. Maller, Trends Food Sci. Tech. 1998, 9, 28.
7. C.O.A. Olsson, D. Landolt, Electrochim. Acta. 2003, 48, 1093.
8. R. Robin, F. Miserque, V. Spagnol, J. Nucl. Mater. 2008, 375, 65.
9. N. Padhy, S. Ningshen, B.K. Panigrahi, U. Kamachi Mudali, Corros. Sci. 2010, 52, 104.
10. V. Kain, S. S. Shinde, H. S. Gadiyar, J. Mater. Eng. Perform. 1994, 3, 699.
11. D. Wallinder, J. Pan, C. Leygraf, A. Delblanc-Bauer, Corros. Sci. 1999, 41, 275.
12. I. Olefjord, Wegrelius, Corros. Sci. 1990, 31, 89.
13. G. Rondelli, P. Torricelli, M. Fini, R. Giardino, Biomaterials, 2005, 26, 739.
14. W. P. Yang, D. Costa, P. Marcus. J. Electrochem. Soc. 1994, 141, 2669.
15. C. F. Dong, A. Q. Fu, X. G. Li, Y. F. Cheng, Electrochim. Acta. 2008, 54, 628.
16. M. Sluyters-Rehbach, Pure & Appl. Chem. 1994, 66, 1831.
17. A.K. Shukla, R. Balasubramaniam, S. Bhargava, Intermetallics. 2005, 13, 631.
18. Z. Grubac, M. Metikos-Hukovic, J. Electroanal. Chem. 2004, 565, 85.
19. D.B. Camovska, M. Lj. Arsov, T. P. Grcev, Maced. J. Chem. Chem. Eng. 2007, 26, 95.
20. A. Popova, S. Raicheva, E. Sokolova, M. Christov, Langmuir. 1996, 12, 2083.
21. T. P. Cheng, J. T. Lee, W. T. Tsai, Electrochim. Acta. 1991, 36, 2069.
22. L-F.Li, P.Caenen, J-P.Celis, J. Electrochem Soc. 2005, 152, B352.
23. J. T. Zhang, J. M. Hu, J. Q. Zhang, C. N. Cao, Prog. Org. Coating. 2004, 51, 145.
24. NIST X-ray Photoelectron Spectroscopy Database, NIST Standard Reference Database 20, Version 3.5, http://srdata.nist.gov/xps.
25. S. Ningshen, U. Kamachi Mudali, G. Amerendra, Baldev Raj, Corros. Sci. 2009, 51, 322.
26. ASTM International A 967-05, Standard Specification for Chemical Passivation Treatments for Stainless Steel Parts.
27. ASTM International, A 380-06, Standard Practice for Cleaning, Descaling, and Passivation of Stainless Steel Parts, Equipment, and Systems.
28. A.A. Hermas, Corrosion Sci. 2008, 50, 2498.
29. E. Barsoukov, J. R. Macdonald, Impedance Spectroscopy: Theory, Experiment, and Applications, 2nd Ed., John Wiley & Sons, NJ, USA, 2005.
30. G. Henkel, B. Henkel, www.henkel-epol.com, Essay No. 45/Rev. 00, 2003.

JCSE The Journal of Corrosion Science and Engineering
ISSN 1466-8858 Volume 15, Preprint 32 submitted 7 July 2012

Table 1. Fitting parameters for the EIS data obtained for different immersion times using the Randle's circuit.

Immersion Times	R_s (Ω/cm^2)	Q_{pf} (S.s^n/cm^2)	n	R_{pf} (Ω/cm^2)
5 minutes	0.5985	5.223×10^{-5}	0.9412	3.98×10^{4}
15 minutes	0.5973	4.964×10^{-5}	0.9381	6.02×10^{4}
30 minutes	0.6029	4.715×10^{-5}	0.9414	8.30×10^{4}
1 hour	0.6121	4.417×10^{-5}	0.9446	1.29×10^{5}
2 hours	0.6173	4.223×10^{-5}	0.9462	1.95×10^{5}
4 hours	0.6225	4.069×10^{-5}	0.9469	3.08×10^{5}
10 hours	0.6304	3.896×10^{-5}	0.9472	5.53×10^{5}
1 day	0.6266	3.679×10^{-5}	0.9470	7.02×10^{5}
3 days	0.5917	3.603×10^{-5}	0.9397	1.08×10^{6}
4 days	0.5835	3.583×10^{-5}	0.9385	1.14×10^{6}
5 days	0.5644	3.553×10^{-5}	0.9392	1.15×10^{6}

JCSE The Journal of Corrosion Science and Engineering
ISSN 1466-8858 Volume 15, Preprint 32 submitted 7 July 2012

Table 2. XPS peak position and peak area for the sample immersed in 5M HNO_3.

Immersion Time	Spectra	Position (ev)	Peak Area (area unit)	FWHM (ev)	Gaussian-Lorentzian (%)
As-polished	Cr $2p_{3/2}$ (met)	573.95	533.19	1.22	0
	$Cr^{3+}2p_{3/2}$ (ox)	576.65	3023.63	3.28	0
	Cr $2p_{1/2}$ (met)	583.18	219.08	1.15	80
	$Cr^{3+}2p_{1/2}$ (ox)	586.47	1367.82	2.6	80
	Fe $2p_{3/2}$ (met)	706.81	447.19	0.77	0
	$Fe^{2+}2p_{3/2}$ (ox)	709.91	1963.92	4.64	1
	Fe $2p_{1/2}$ (met)	719.65	170.47	1.12	0
	$Fe^{2+}2p_{1/2}$ (ox)	722.91	258.57	3.01	0
	Ni $2p_{3/2}$ (met)	852.79	391.18	1.12	0
	$Ni^{3+}2p_{3/2}$ (ox)	855.81	80.43	0.96	90
5 minutes	Cr $2p_{3/2}$ (met)	573.91	1367.82	1.18	0
	$Cr^{3+}2p_{3/2}$ (ox)	576.65	3046.74	3.14	0
	Cr $2p_{1/2}$ (met)	583.22	132.14	1.17	0
	$Cr^{3+}2p_{1/2}$ (ox)	586.45	1050.46	3.35	0
	Fe $2p_{3/2}$ (met)	706.83	820.02	0.76	0
	$Fe^{2+}2p_{3/2}$ (ox)	709.30	1771.68	4.81	0
	Fe $2p_{1/2}$ (met)	719.80	532.02	1.28	26
	$Fe^{2+}2p_{1/2}$ (ox)	722.06	286.88	3.82	0
	$Ni2p_{3/2}$ (met)	852.79	421.06	0.87	80
15 minutes	Cr $2p_{3/2}$ (met)	573.86	495.65	1.22	0
	$Cr^{3+}2p_{3/2}$ (ox)	576.71	3237.48	3.06	0
	Cr $2p_{1/2}$ (met)	583.17	134.22	1.26	0
	$Cr^{3+}2p_{1/2}$ (ox)	586.61	1705.10	3.39	36
	Fe $2p_{3/2}$ (met)	706.83	820.54	0.8	0
	$Fe^{2+}2p_{3/2}$ (ox)	709.30	1771.60	4.29	25
	Fe $2p_{1/2}$ (met)	719.74	310.65	1.12	2
	Fe^{2+} $2p_{1/2}$ (ox)	722.36	131.57	3.81	0
	Ni $2p_{3/2}$ (met)	852.79	421.06	0.87	80
1 day	Cr $2p_{3/2}$ (met)	573.78	296.63	0.95	0
	$Cr^{3+}2p_{3/2}$ (ox)	576.52	3606.35	2.93	8
	Cr $2p_{1/2}$ (met)	583.16	138.91	1.25	0
	$Cr^{3+}2p_{1/2}$ (ox)	586.40	1808.62	3.27	0
	Fe $2p_{3/2}$ (met)	706.85	922.83	0.81	3
	$Fe^{2+}2p_{3/2}$ (ox)	709.29	1651.56	4.97	0
	Fe $2p_{1/2}$ (met)	719.85	453.70	1.4	0
	$Fe^{2+}2p_{1/2}$ (ox)	722.30	261.08	4.6	0
	Ni $2p_{3/2}$ (met)	852.71	662.17	1.05	35
5 days	Cr $2p_{3/2}$ (met)	573.83	237.25	0.93	0
	$Cr^{3+}2p_{3/2}$ (ox)	576.63	3801.10	2.91	13
	Cr $2p_{1/2}$ (met)	583.28	133.01	1.38	0
	$Cr^{3+}2p_{1/2}$ (ox)	586.49	1836.88	3.26	0
	Fe $2p_{3/2}$ (met)	706.89	915.68	0.82	6
	$Fe^{2+}2p_{3/2}$ (ox)	709.38	1920.09	4.94	0
	Fe $2p_{1/2}$ (met)	719.84	451.56	1.63	0
	Ni $2p_{3/2}$ (met)	852.91	665.95	1.04	44

JCSE The Journal of Corrosion Science and Engineering
ISSN 1466-8858 Volume 15, Preprint 32 submitted 7 July 2012

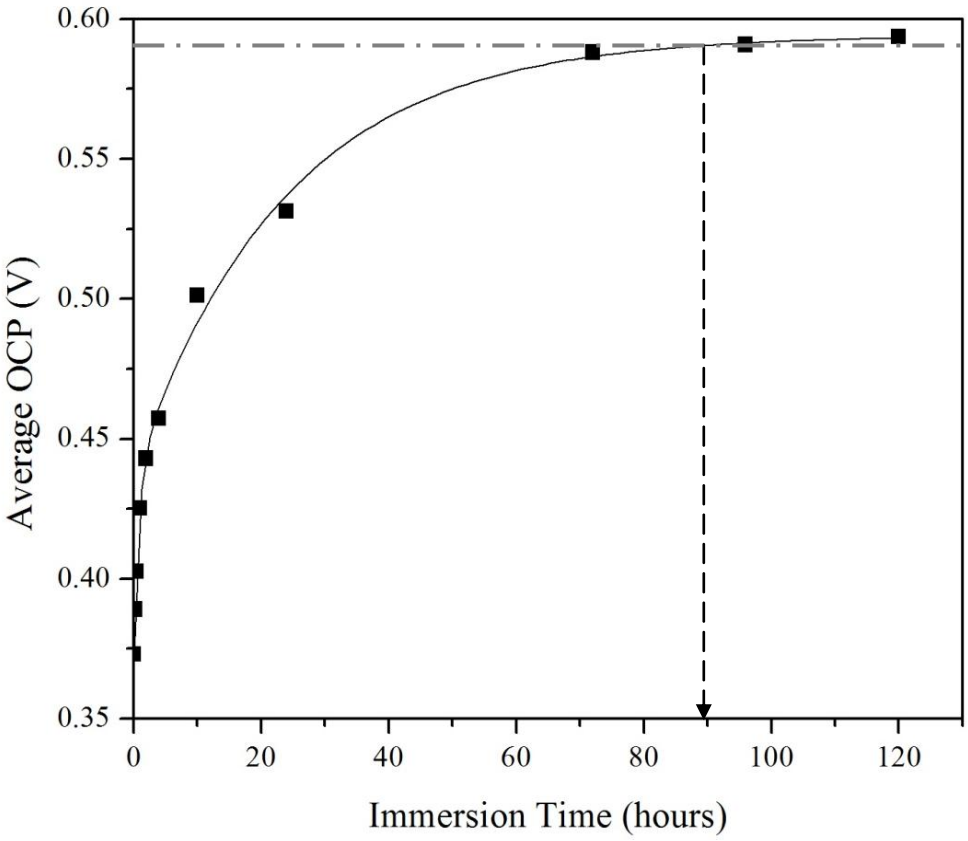

Fig. 1. Open circuit potential values for samples immersed in 5M HNO_3 versus immersion time at room temperature.

JCSE The Journal of Corrosion Science and Engineering
ISSN 1466-8858 Volume 15, Preprint 32 submitted 7 July 2012

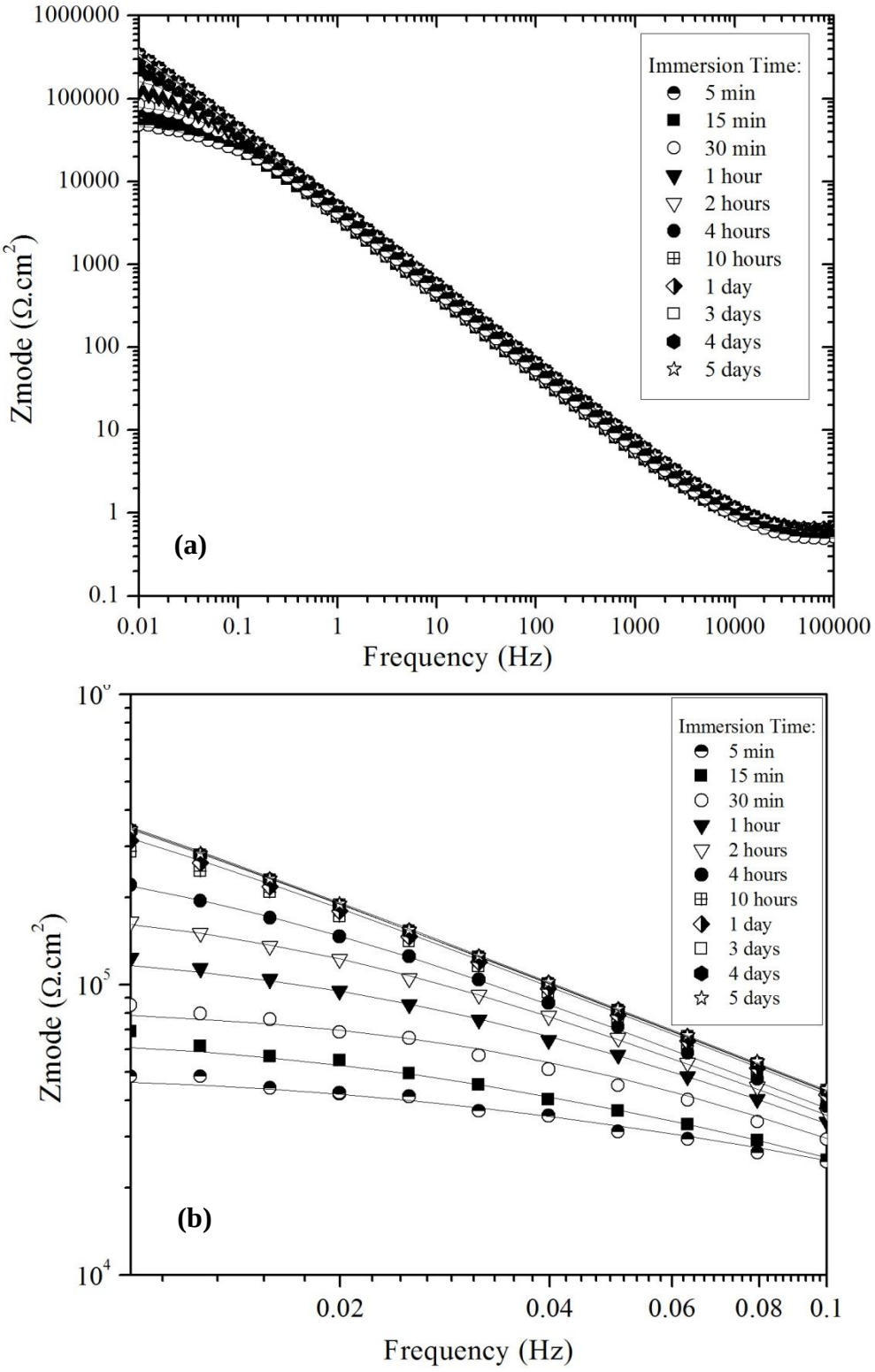

Fig. 2. a) Bode magnitude plots of EIS data in 5M HNO_3 solution at room temperature for different immersion times. b) The low frequency region at a different scale. (Lines: Fitted data; Symbols: Experimental data)

JCSE The Journal of Corrosion Science and Engineering
ISSN 1466-8858 Volume 15, Preprint 32 submitted 7 July 2012

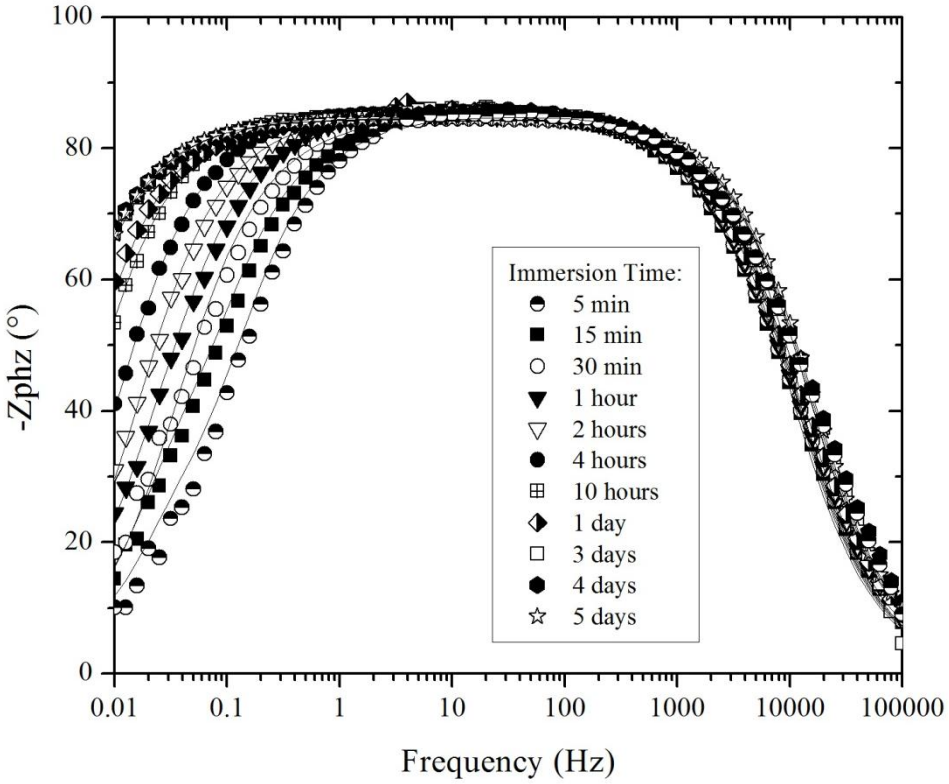

Fig. 3. Bode phase angle plots of EIS data in 5M HNO_3 solution at room temperature for different immersion times. (Lines: Fitted data; Symbols: Experimental data)

JCSE The Journal of Corrosion Science and Engineering
ISSN 1466-8858 Volume 15, Preprint 32 submitted 7 July 2012

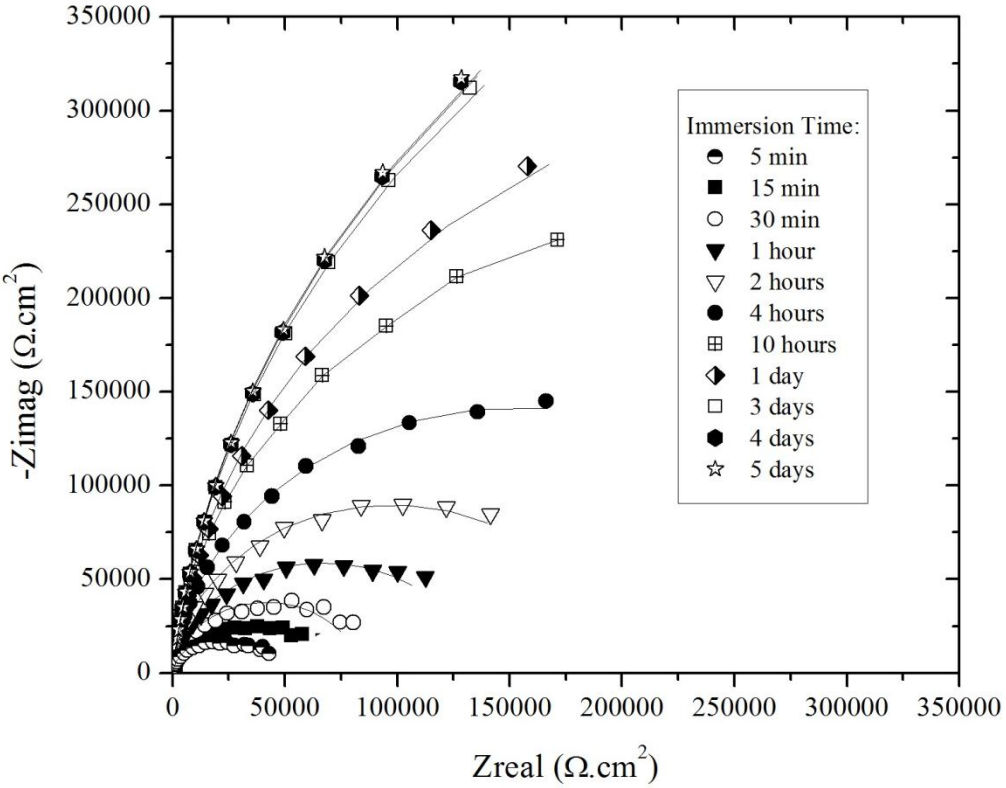

Fig. 4. Nyquist plots of EIS data in 5M HNO_3 solution at room temperature and different immersion times. (Lines: Fitted data; Symbols: Experimental data).

JCSE The Journal of Corrosion Science and Engineering
ISSN 1466-8858 Volume 15, Preprint 32 submitted 7 July 2012

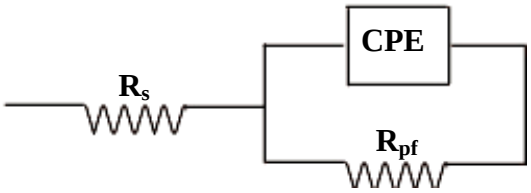

Fig. 5. Equivalent electric circuit to model EIS experimental data.

JCSE The Journal of Corrosion Science and Engineering
ISSN 1466-8858 Volume 15, Preprint 32 submitted 7 July 2012

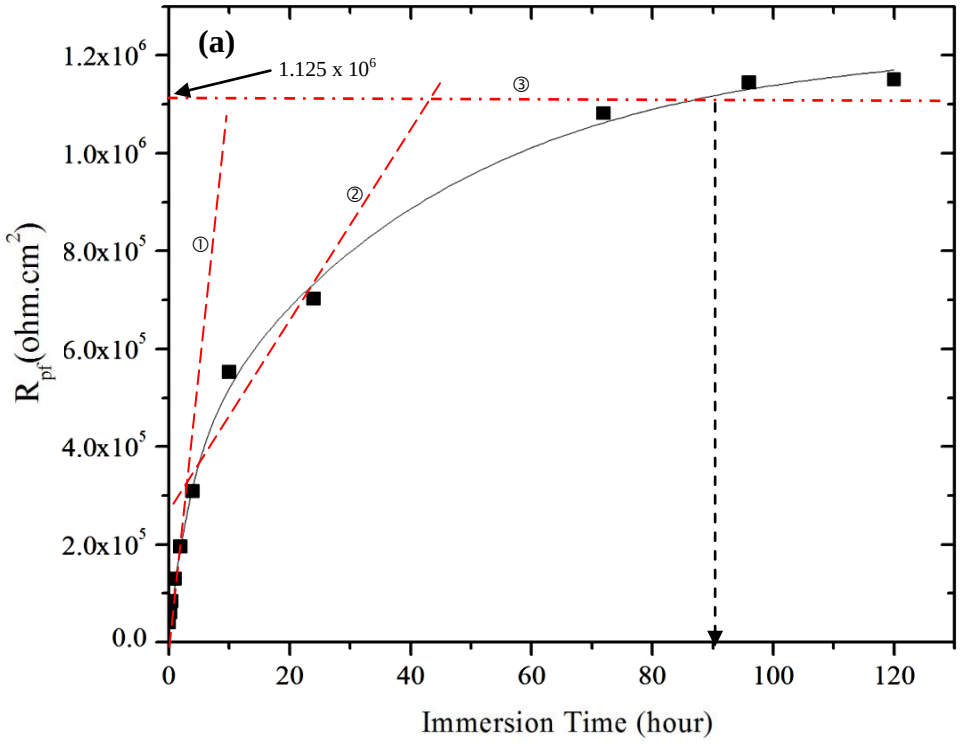

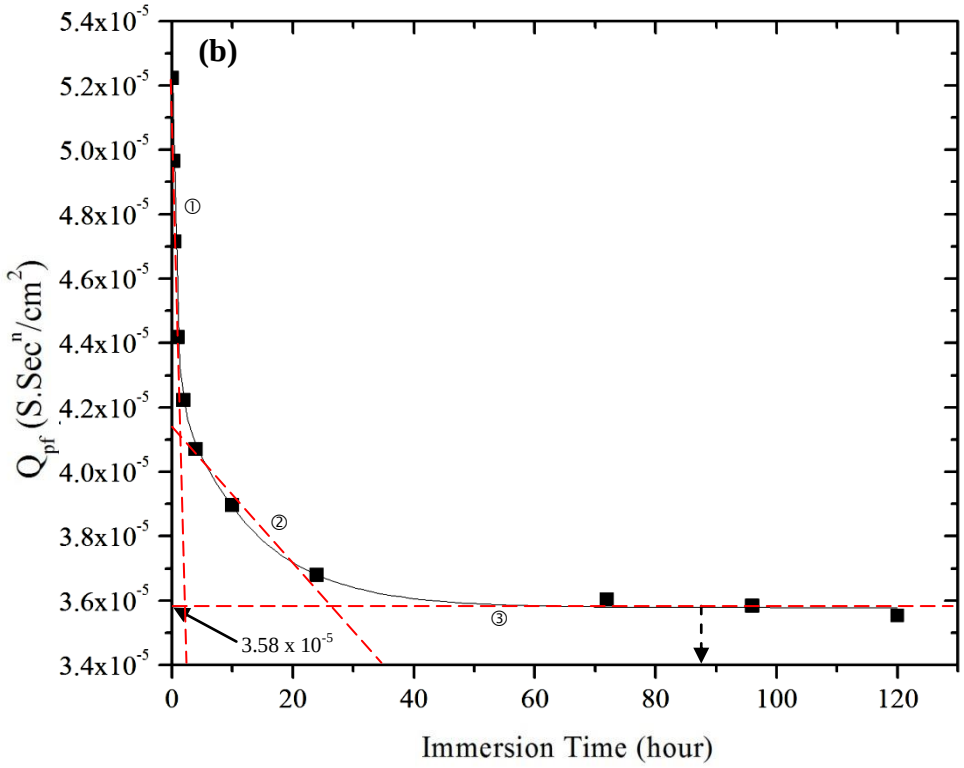

Fig. 6. Resistance (a) and CPE values (b) of the passive film for different immersion times. Room temperature.

JCSE The Journal of Corrosion Science and Engineering
ISSN 1466-8858 Volume 15, Preprint 32 submitted 7 July 2012

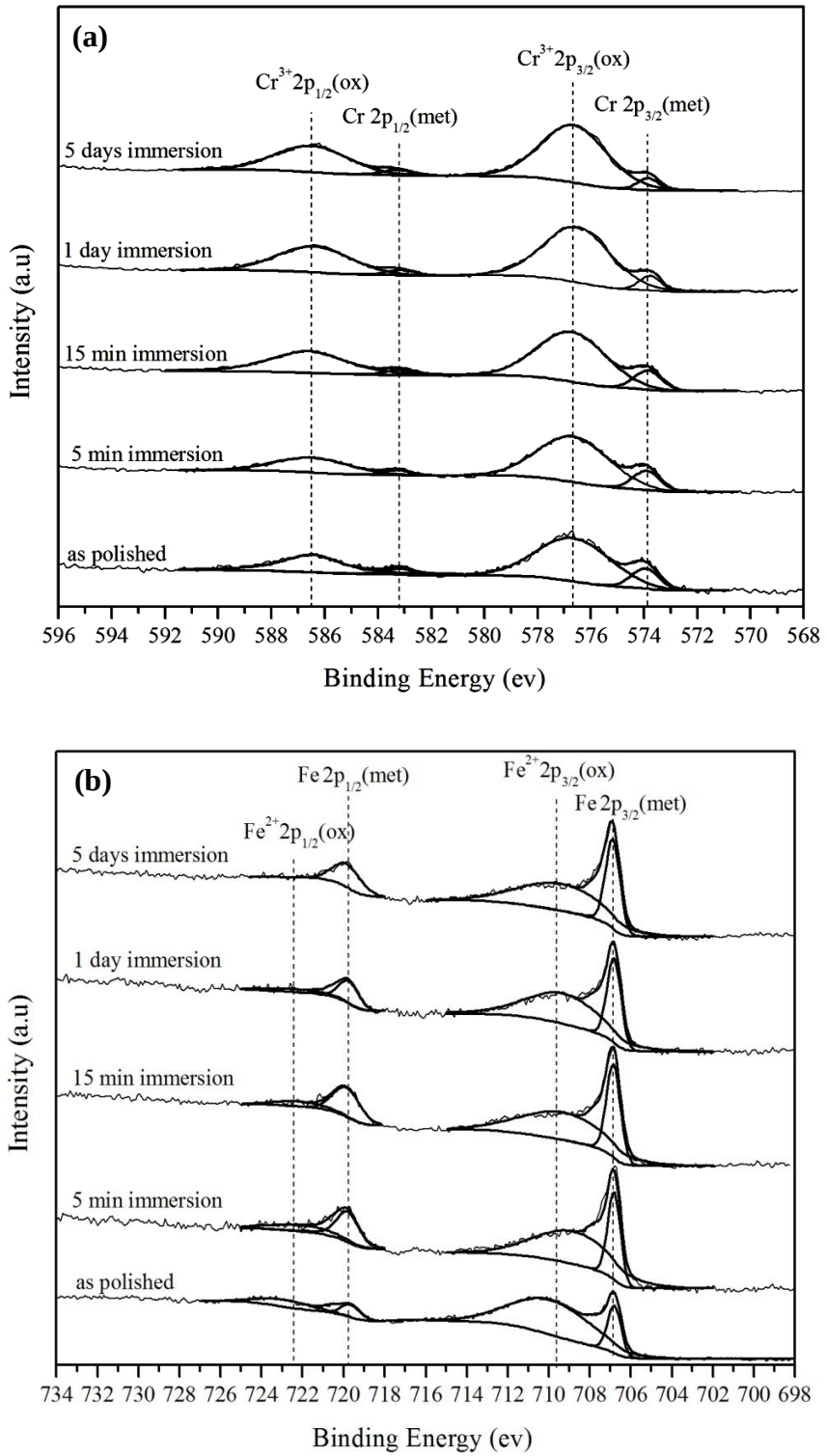

Fig. 7. (a) Cr and (b) Fe 2p spectra recorded for as polished samples and the samples immersed in 5M HNO_3 solution for 5min, 15min, 1 day and 5 days. The tests were conducted at room temperature.

JCSE The Journal of Corrosion Science and Engineering
ISSN 1466-8858 Volume 15, Preprint 32 submitted 7 July 2012

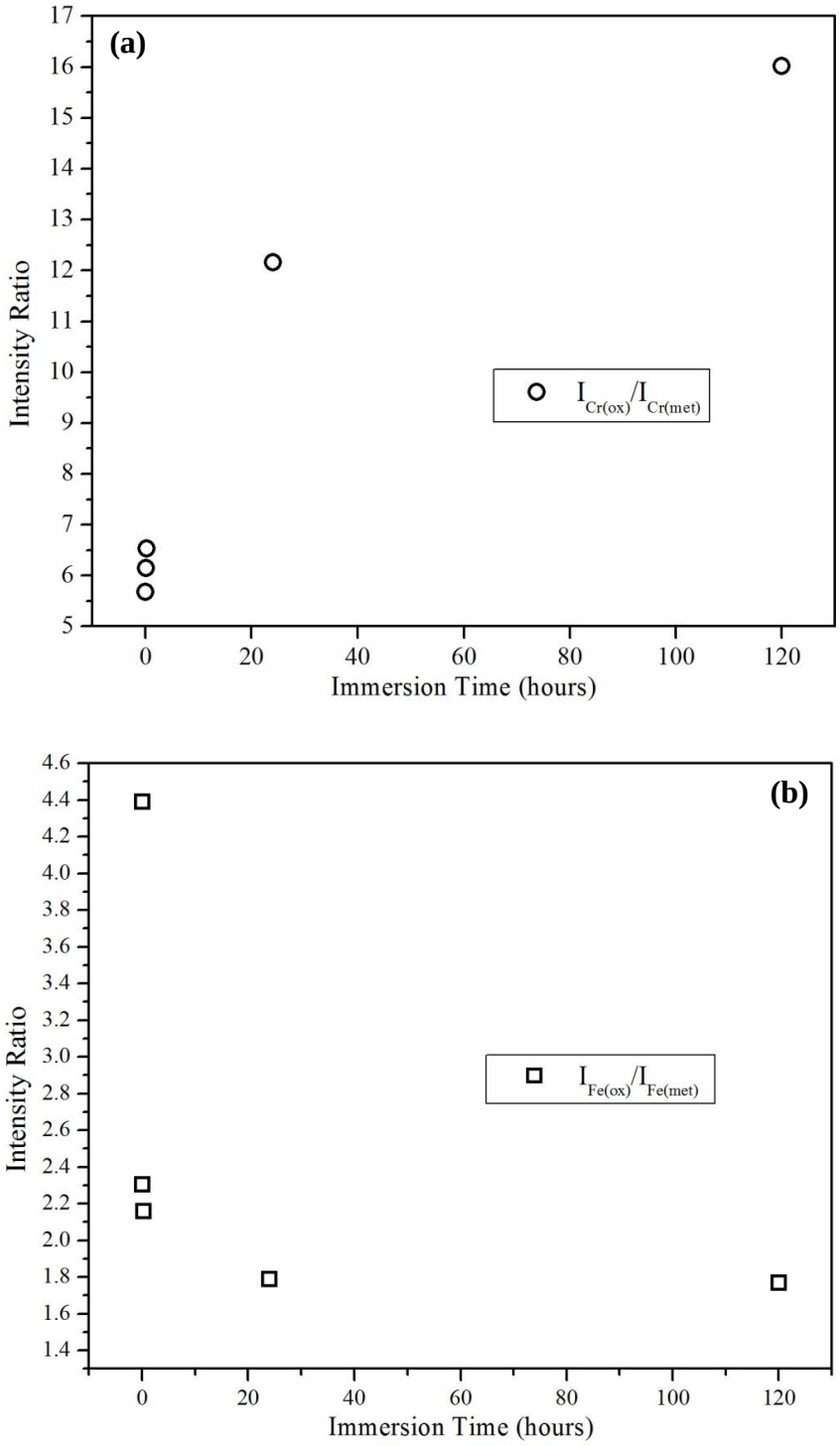

Fig. 8. Oxide to metal ratio for the $2p_{3/2}$ spectra of (a) Cr and (b) Fe of the as-polished samples and samples immersed in 5M HNO_3 solution for 5 min, 15 min, 1 day and 5 days at room temperature.

JCSE The Journal of Corrosion Science and Engineering
ISSN 1466-8858 Volume 15, Preprint 32 submitted 7 July 2012

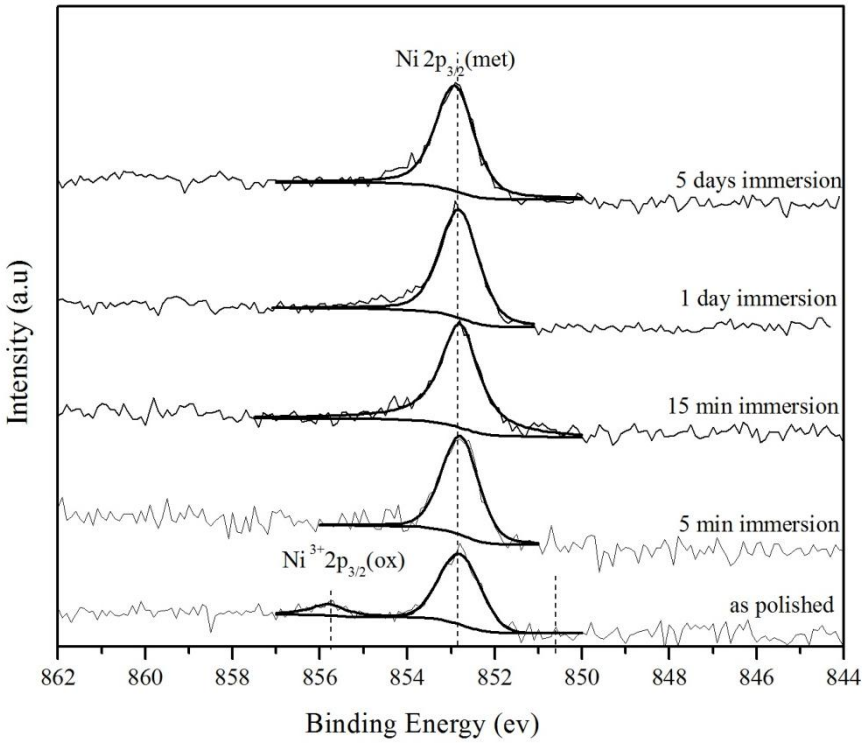

Fig. 9. Ni 2p spectra for as the polished sample and the samples immersed in the 5M HNO_3 solution at room temperature for 5min, 15min, 1 day and 5 days.